Composite Interfaces, 2013
Vol. 20, No. 4, 287–298, http://dx.doi.org/10.1080/15685543.2013.796753

Liquid crystalline single-polymer short-fibers composites

Thiago Medeiros Araujo* and Alessandro Pegoretti

Department of Industrial Engineering, University of Trento, Trento, Italy

(*Received 27 February 2013; accepted 15 April 2013*)

Single-polymer short-fibers composites (SPSFCs) were obtained by including Vectran® fibers in a Vectran® matrix. A thermal annealing treatment was optimized to increase the melting temperature, mechanical properties, and thermal stability of pristine Vectran® fibers, and a two-step process was successfully developed to consolidate SPSFCs containing up to 30 wt.% of reinforcement. The composites exhibited a remarkable improvement of the tensile modulus (up to 161%) and a decrease of elongation at break in comparison with the unfilled matrix. A slight decrease of the composites tensile strength was also observed which suggested an investigation of the matrix–reinforcement interfacial adhesion. SEM observations evidenced some pull-out phenomena, indicating a poor interfacial adhesion. A plasma surface treatment on the reinforcing fibers was performed in order to increase the interfacial adhesion in the composites. The results showed an increase of almost 180% in the tensile modulus compared with the unfilled matrix and fiber breakage as main fracture mechanism.

Keywords: single-polymer composites; liquid crystalline polymer; Vectran®; mechanical properties

1. Introduction

Due to an increasing attention to environment preservation and the introduction of specific regulations, a general need to improve the recyclability of composites materials has recently emerged. In order to fulfill this new requirement, the development of so-called single-polymer composites (SPCs) or self-reinforced composites, i.e. composite materials in which both matrix and reinforcement have the same chemical composition has received certain stimulus.[1] Unlike traditional heterogeneous composites (such as glass- or carbon-reinforced thermosettings), SPCs can be entirely melted down at the end of the product life for recycling. On the other hand, one of the main challenges in the SPCs production is the small melting temperature difference generally existing between fiber and matrix of the same chemical nature.[2,3]

Liquid crystalline polymers (LCPs) represent a class of polymers well known for their excellent mechanical properties, thermal and chemical resistance, and low density which result in outstanding specific properties.[4] Unlike conventional polymers, they crystallize from an ordered and oriented molecular phase intermediate between an isotropic liquid phase and a crystalline solid, or an amorphous glassy phase. Ordered liquid crystalline phases are mainly classified as nematic, cholesteric, and smectic and

*Corresponding author. Email: thiago.medeiros@ing.unitn.it

the structural basis for each of them is a state of matter in which the degree of molecular order is intermediate between the perfect three-dimensional, long-range positional, and orientational order found in solid crystals and the absence of long-range order found in isotropic liquids, gases, and amorphous solids called as mesomorphic state. [5–7] LCPs can be broadly classified into three classes: (a) aromatic polyamides, (b) aromatic heterocycles, and (c) aromatic copolyesters.[4] Aromatic polyamide fibers, commonly known as aramid fibers, are obtained from polyamides containing aromatic rings along the main chain: the most known commercial products are Kevlar®, and Twaron®. Aromatic heterocyclic polymers represent themselves lyotropic materials and are characterized by wholly aromatic molecular structures with fused heterocyclic rings along the main chain; PBI and Zylon® are two examples in this category. Aromatic copolyester polymers possess thermotropic behavior and are characterized by molecular structure with a high degree of linearity and rigidity that allow the formation of ordered phases over a wide temperature range; among them, Vectra®, Xydar®, and Ekonol®.[4] In particular, Vectran® is a copolymer of 4-hydroxybenzoic acid (HBA) and 6-hydroxy-2-naphthoic acid (HNA) with a molar ratio of 73/27, respectively. The melt-spun Vectra-based fiber, commercially known as Vectran®, is superior to aramid fibers in several ways: it is highly resistant to creep, it resists flex or fold fatigue and abrasion, and has better long-term resistance to UV degradation.[6,8]

Previous investigations have shown that single-polymer long-fiber composites can be successfully produced using commercially available continuous LCP fibers having different thermal transitions.[9–11] The aim of this work is to investigate the possibility to produce single-polymer short-fibers composites using Vectran® fibers and to quantify their thermo-mechanical response.

2. Experimental

2.1. Materials and sample preparation

The starting material is a commercially available Vectran® NT fiber (Kuraray) having a linear density of 750 denier and 150 filaments per yarn. According to the material data sheet, a weaving finish was applied at a level of ~0.5% oil-on-yarn to assist processing (e.g. rewinding, twisting, braiding, and weaving). The fibers have an almost circular cross-section with an average diameter of 25.5 ± 2.1 μm. Continuous Vectran® NT fibers have been chopped in 12 mm short fibers using a fiber chopper model B-410 (Glascraft Composites Equipment). In order to avoid their melting during melt-compounding in a matrix of Vectran® NT, heat treatment was optimized in order to increase their melting temperature (and tensile properties). In particular, annealing thermal treatments were performed on Vectran® NT fibers in an oven under inert atmosphere in the temperature range from 240 to 300 °C and treatment times between 2 and 24 h.

Single-polymer short-fibers composites (SPSFCs) were prepared by a two-step process. In the first step, as-received Vectran® fibers were mechanically mixed with thermally annealed Vectran® fibers at weight fractions of 10, 20, and 30%. The mixture was placed between two 1 mm thick PTFE sheets and hot-pressed in an aluminum square mold of 120 mm × 120 mm and 1 mm thick using a Carver laboratory press. A proper temperature (295 °C) between the melting points of the constituents was selected for the consolidation process performed at a pressure of 4.4 MPa for 30 s. Then, SPSFCs were cooled under pressure (1.8 MPa). The unfilled matrix plates used for comparison purposes were prepared using the same processing and consolidation route without the addition of reinforcement.

2.2. Experimental techniques

Differential scanning calorimetry (DSC) measurements were performed using a Mettler DSC 30 Low Temperature Cell and a Mettler TC 15 TA Controller at a heating rate of 10 °C/min under a nitrogen flux of 100 mL/min.

All tensile tests were conducted using a universal testing machine (Instron, model 4502). Tensile tests on the single fibers were executed according to ASTM standard D3379 with a 10 N load cell. Single fibers were randomly extracted from a bundle and mounted on window cards using a quick-setting glue. The diameter of individual fibers was measured using an optical microscope. The gage length was fixed at 25 mm and the cross-head speed at 1 mm/min.

Tensile tests on composites were performed according to ISO 527 on 1BA specimens with a gage length of 25 mm, at a cross-head speed of 1 mm/min with a 1 kN load cell. The strain was recorded by using a resistance extensometer Instron model 2620-601 with a gage length of 12.5 mm.

Dynamic mechanical thermal analysis (DMTA) under tensile configuration was performed by a DMA Q800 (TA Instruments, New Castle, USA) apparatus on rectangular specimens of 5 mm × 15 mm × 1 mm at a frequency of 1 Hz. Storage modulus E' and loss tangent ($\tan\delta$) were determined in the temperature range from 0 °C to 200 °C. A peak-to-peak displacement of 64 μm and a heating rate of 3 °C/min were imposed.

Field emission scanning electron microscopy (FESEM) images were obtained using a Supra 40 (Zeiss) microscope with the operating mode in high vacuum and secondary electron detector.

2.3. Plasma treatment

A plasma apparatus, consisting of a glass cylinder reactor (500 mm in length and 150 mm in diameter) equipped with semi-cylindrical copper electrodes, was assembled in this laboratory. A radiofrequency generator RF5S (maximum power 500 W and frequency 13.56 MHz) matching network AM-5 and controller AMNPS-2A supplied by RF Plasma Products (Marlton, NJ, USA) were used. Vacuum produced by a double stage pump was controlled and measured by Edwards devices. The working pressure was about 1 atmosphere. The voltage of 30 V and treatment time of 3 min were used for fibers treatment; oxygen fluxed along the reactor axis at a flow rate of 10 ml/min.

3. Results and discussion

3.1. Thermal analysis

In the past two decades, thermal annealing treatments of liquid crystalline nematic random copolymers were widely studied.[12] Depending on the annealing conditions, an endotherm peak may appear at temperatures lower than the annealing temperature. Economy et al. [13] show that upon annealing at temperatures higher than the crystal-to-nematic transition (TCN) a chemical randomization occurs through transesterification. The annealing treatment used in the present work was motivated by the previous treatments successfully developed for commercial Vectran® fibers.[12,14–16]

To understand the influence of the annealing temperature, DSC analysis on fibers treated at 240 °C, 260 °C, 280 °C, and 300 °C for 2 h were performed. As it can be observed in Figure 1a, the thermograms of untreated fibers present two wide endothermal peaks (Tp_1 and Tp_2), probably related to an orthorhombic to nematic transition.

[15,17,18] After the thermal annealing treatment, a new endothermic peak (Tm_1) appears at a temperature increasing with the annealing temperature. As reported in previous studies, Tm_1 could be attributed to inter-chain transesterification reactions. [13,17,18] When the treatment was performed at 300 °C, Tm_1 overlaps the endothermic peaks Tp_1 and Tp_2 present in the untreated fibers become the new transition temperatures of the fibers. Due to a largest increment in Tm_1 temperature, 300 °C was chosen as heat-treatment temperature. In order to establish an optimal treatment time, DSC analysis were also performed on fibers treated at 300 °C for 2, 6, 9, 12, 15, 19, and 24 h. The DSC traces of Vectran® fibers as a function of treatment time at 300 °C are presented in Figure 1b. It is interesting to observe that until 15 h of treatment, Tm_1 moves to higher temperatures with increasing treatment times. After this time, Tm_1 starts to decrease, probably due to concurrent degradative phenomena. The annealing at

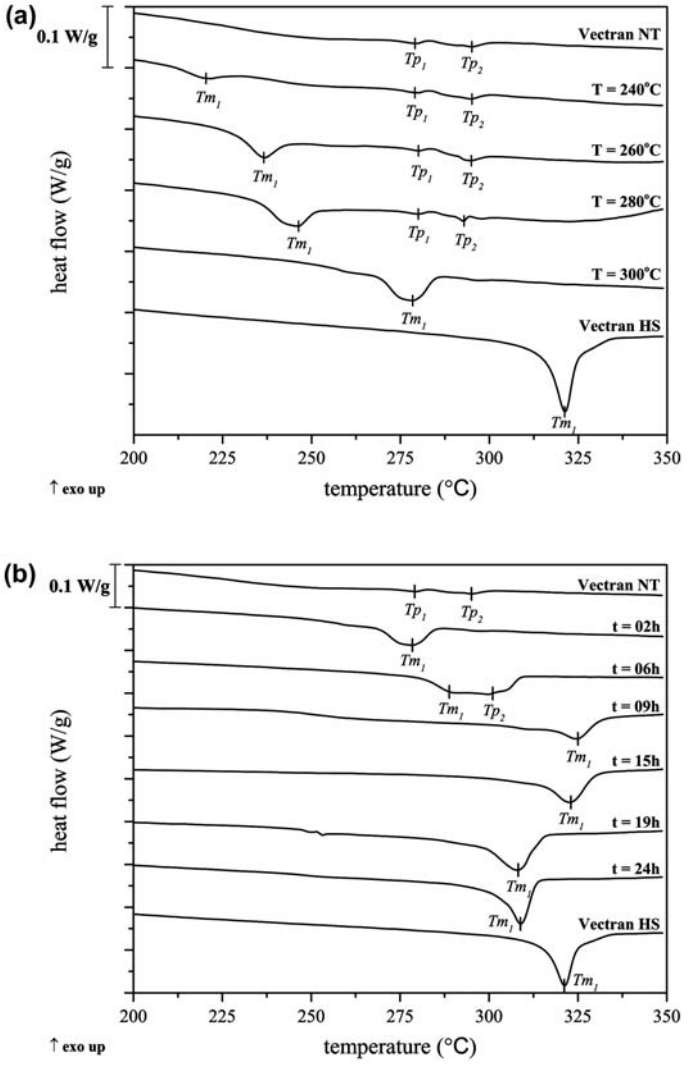

Figure 1. DSC traces on Vectran® fibers as a function of (a) annealing temperature for 2 h and (b) annealing duration at 300 °C.

300 °C for 15 h in inert atmosphere effectively increased the melting point of Vectran® NT fibers by almost 30 °C. Therefore, these conditions were selected for an optimal treatment. For comparison purposes, on both Figure 1a and b, the thermogram of commercially available Vectran® HS fibers is reported. Vectran® HS fibers have been subject to a proprietary heat treatment under tension.[19]

3.2. Microstructure

FESEM micrographs of fracture surfaces of SPSFCs filled with 20 wt.% of annealed fibers, and plasma-treated annealed fibers are reported in Figure 2. First of all, it is important to note that due to proper thermal annealing, the fibers are able to maintain their structure and appear to be homogenously surrounded by a polymeric matrix generated by the melting of the as-received Vectran® NT fibers. This confirms the suitability of the selected processing conditions to generate a short-fiber reinforced single-polymer composite based on liquid crystalline polymer. It also interesting to observe that Figure 2(a) and (b) shows the presence of distributed pull-out phenomena instead of fibers breakage, thus, indicating the existence of a poor fiber–matrix interface. On the other hand, the fracture surface of SPSFC filled with 20 wt.% plasma-treated annealed fibers (Figure 2c) show mostly fiber breakage phenomena attesting the improvement in terms of interfacial adhesion between matrix and reinforcement.

3.3. Mechanical properties

Table 1 compares the mechanical properties of as-received and annealed single-fibers. It is worthwhile to observe that besides an increment in the melting temperature, the annealing treatment of the fibers increases their tensile strength by 51% and elongation at break by 16% in comparison with as-received Vectran® NT fiber. However, the tensile modulus of the fibers does not change significantly. The improvement on the tensile properties of LCP fibers has been attributed to the increase in molecular weight after the treatment due to the transesterification reactions induced by thermal annealing.[14,15]

Table 2 compares the tensile properties of the unfilled matrix with the composites produced with different weight fractions of reinforcement. It is worthwhile to note that composites with 10 wt.% of reinforcement do not manifest a significantly improvement of the tensile properties. On the other hand, when the reinforcement is raised to 20 wt.%, the tensile modulus increases by 35% and with a further increment in the reinforcement content (up to 30 wt.%), a noticeable increment of 161% in the tensile modulus can be observed. At the same time, all the investigated SPSFCs manifest a decrease in the elongation at break with respect to the unfilled matrix. The tensile strength does not show significant variations with the amount of reinforcement.

According to FESEM observations (see Figure 2c), a poor interfacial adhesion was evidenced when annealed fibers were used. This behavior could be tentatively explained by considering the presence of a finishing on the Vectran® NT fibers. The finishing is added to the fibers during their production with the aim to compact the yarns and favor the typical processes adopted for composite manufacturing. The presence of such sizing may be the cause of the poor interfacial adhesion observed; also chemical changes could occur in the sizing during the heat treatment developed in this work, hindering a good matrix–fiber interface. To preserve the SPCs concept, the use of coupling agents was avoided and a surface plasma treatment was preferred.

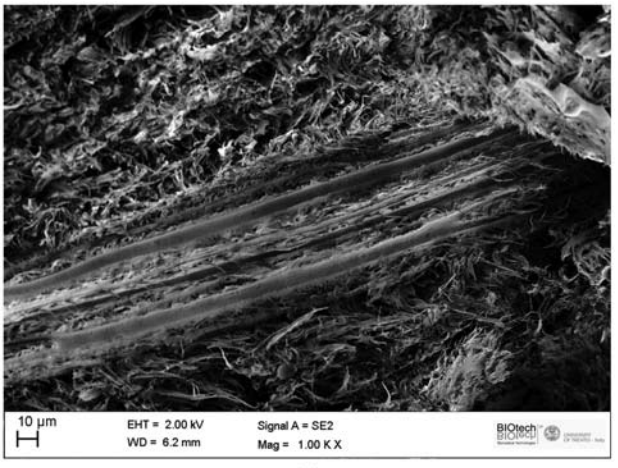

(a)

(b)

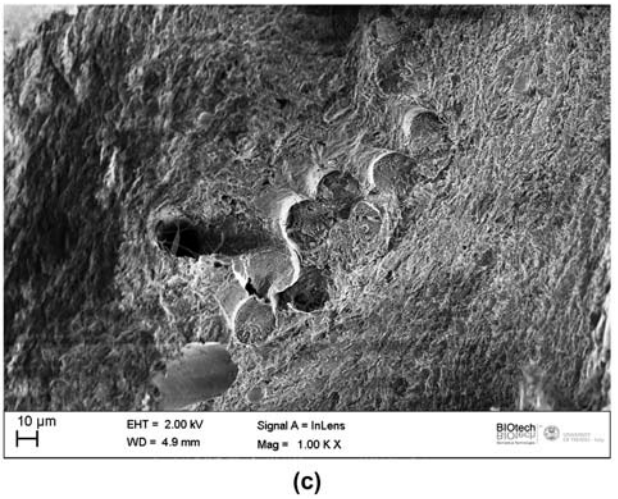

(c)

Figure 2. FESEM micrographs of fracture surfaces of SPSFCs filled with 20 wt.% of annealed fibers (a) and (b), and (c) plasma-treated annealed fibers.

Table 1. Results of single-fiber tensile tests on as-received and annealed Vectran® NT fibers.

Property	As received fibers	Annealed fibers
Tensile modulus [GPa]	61.6 ± 3.2	61.4 ± 8.8
Tensile strength [MPa]	1006.9 ± 43.8	1521.1 ± 123.1
Elongation at break [%]	2.17 ± 0.15	2.43 ± 0.23

Table 2. Tensile properties of unfilled matrix and SPSFCs at different weight fractions of annealed Vectran® NT fibers.

Property	Unfilled matrix	SPSFC (10 wt.%)	SPSFC (20 wt.%)	SPSFC (30 wt.%)
Tensile modulus [GPa]	1.31 ± 0.14	1.30 ± 0.12	1.77 ± 0.10	3.42 ± 0.67
Tensile strength [MPa]	37.7 ± 9.2	33.8 ± 5.6	33.2 ± 4.6	29.3 ± 4.0
Elongation at break [%]	5.00 ± 1.44	3.71 ± 0.77	2.59 ± 0.56	0.79 ± 0.20

Table 3. Tensile properties of unfilled matrix and SPSFC with 20 wt.% of annealed fibers, and annealed fibers with a plasma surface treatment.

Property	Unfilled matrix	Annealed fibers (20 wt.%)	Plasma treated annealed fibers (20 wt.%)
Tensile modulus [GPa]	1.31 ± 0.14	1.77 ± 0.10	3.64 ± 1.30
Tensile strength [MPa]	37.7 ± 9.2	33.2 ± 4.6	31.7 ± 11.0
Elongation at break [%]	5.00 ± 1.44	2.59 ± 0.56	0.73 ± 0.16

The results of the tensile properties on SPSFC containing 20 wt.% of annealed and plasma-treated fibers are summarized in Table 3. A remarkable improvement of 178% in the tensile modulus with respect to the unfilled matrix can be observed. On the other hand, in terms of tensile strength, the composite with plasma-treated fibers maintained the same behavior of the composite with fibers without the plasma treatment. As a predictable result, the elongation at break shows a further decrease in its value since this property is directly related to the fiber/matrix interface thus attesting the efficacy of the plasma treatment. Moreover, FESEM observations confirmed better fiber/matrix compatibility when plasma-treated annealed fibers are used (see Figure 2c).

In order to compare the goodness of the obtained experimental results with theoretical previsional models, the following empirical equations to predict the elastic modulus (E_R) of a composite containing short-fibers randomly oriented in a plane were used.

The first one was proposed by Tsai and Pagano [20],

$$E_R = \frac{3}{8}E_{LL} + \frac{5}{8}E_{TT} \tag{1}$$

the second one was proposed by Cox,[21]

$$E_R = \frac{1}{3}E_{LL} \tag{2}$$

And, the last one was proposed by Loewenstein,[22]

$$E_R = \frac{3}{8}E_{LL} \tag{3}$$

where E_{LL} and E_{TT} represent respectively the longitudinal and transverse tensile moduli for a unidirectional aligned fiber composite having the same fiber volume fraction and fiber aspect ratio of the composite under evaluation and can be estimated by the Halpin–Tsai micromechanics equations [23,24]:

$$E_{LL} = E_m \frac{1 + \zeta_L \eta_L V_f}{1 - \eta_L V_f} \tag{4}$$

$$E_{TT} = E_m \frac{1 + \zeta_T \eta_T V_f}{1 - \eta_T V_f} \tag{5}$$

where E_m is the matrix modulus, V_f is the fiber volume fraction, and:

$$\zeta_L = 2\frac{1}{d} \quad \zeta_L = 2 \quad \eta_L = \frac{\frac{E_f}{E_m} - 1}{\frac{E_f}{E_m} + \zeta_L} \quad \eta_T = \frac{\frac{E_f}{E_m} - 1}{\frac{E_f}{E_m} + \zeta_T} \tag{6}$$

A plot of E_R values estimated in accordance with Equations (1)–(3) and the experimental results as a function of the fiber volume fraction is reported in Figure 3a. It is worthwhile to note that fiber weight and volume fractions assume the same value for SPCs, since fiber and matrix have the same density. It can be observed that the experimental results in terms of tensile modulus are quite far from that (E_R) predicted for a composite material containing short fibers randomly distributed in the plane (2D). The empirical equations (1)–(3) used to obtain the E_R values are based on a two-dimensional composite and good only at very low fiber volume fraction. At high fiber volume fractions, the predicted modulus is much higher than the experimental due to the increase in concentration of defects within the composite increasing the content of fibers.[25] Moreover, the fibers inside the composites produced in this work are randomly oriented through all the composite volume, in other words, the reinforcement present a three-dimensional (3D) orientation. Christensen and Waals [26] proposed the following model to predict the elastic modulus behavior on 3D randomly distributed short-fiber composites;

$$E_R = \frac{V_f}{6}E_f + [1 + (1 + v_m)V_f]E_m \tag{7}$$

where v_m is the Poisson's ratio of the matrix.

A plot of E_R value according to the Christensen and Waals' model (Equation (6)) and the experimental results as a function of the fiber volume fraction is reported in Figure 3b. The experimental value of the elastic modulus of the composite containing

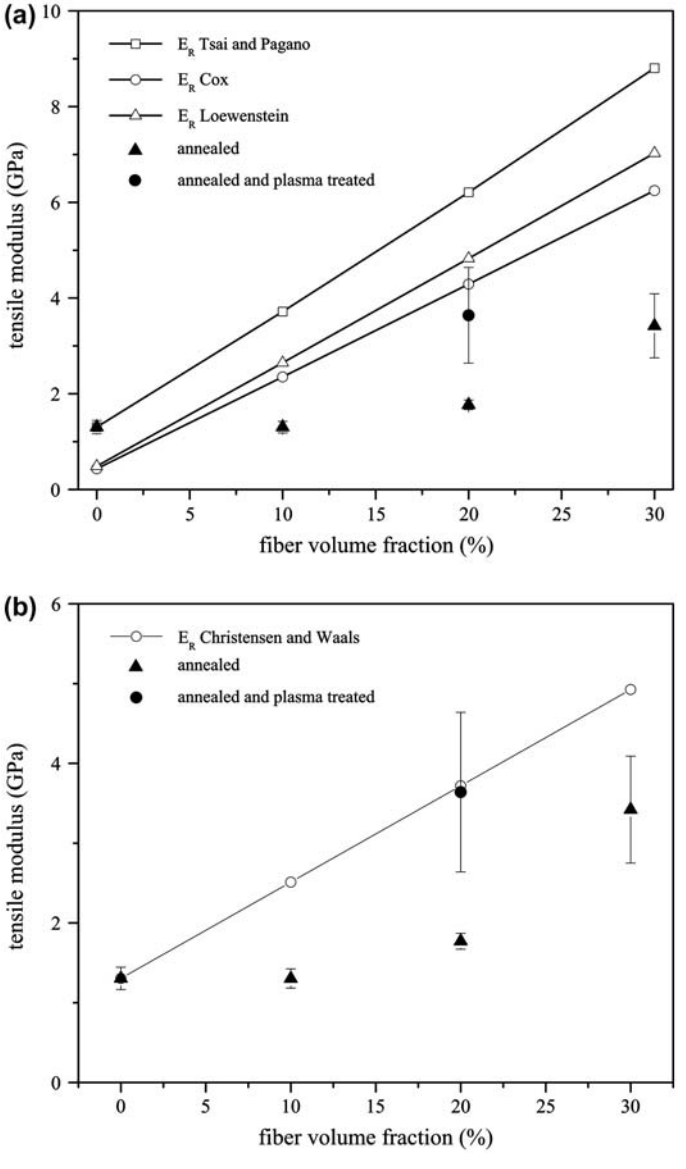

Figure 3. Tensile modulus of SPSFCs containing (▲) annealed and (●) plasma-treated annealed Vectran® fibers. Lines refer to predictive models of Equations (1)–(3) (a) and Christensen and Waals' model (b).

plasma-treated annealed fibers reached the theoretical values E_R proposed by equation (6) attesting once again, the effectiveness of the plasma treatment over the annealed fibers.

In Figure 4a, the storage modulus (E') as function of temperature is reported for neat matrix, and SPSFCs containing various amounts (10, 20, 30 wt.%) of annealed fibers and 20 wt.% of plasma-treated annealed fibers. As the amount of reinforcement

increases, the value of the storage modulus also improves. The composite containing plasma-treated fibers present a higher increment in the storage modulus in comparison with the sample containing the same amount of fibers without surface treatment. This behavior is certainly due to a higher interfacial adhesion between matrix and reinforcement. The tan δ curves are reported in Figure 4b for the same systems. It can be easily noted that tan δ curves do not change substantially with the presence of annealed Vectran® fibers even when they are plasma treated. It is possible to identify two thermal transitions that are generally named α and β. The first one represents the relaxation of the overall chain and corresponds to the beginning of the nematics phase mobility. The second one is attributed to the motions inside the HNA group (C–O bond rotation). [14,27] The β transition does not change its temperature with the addition of the

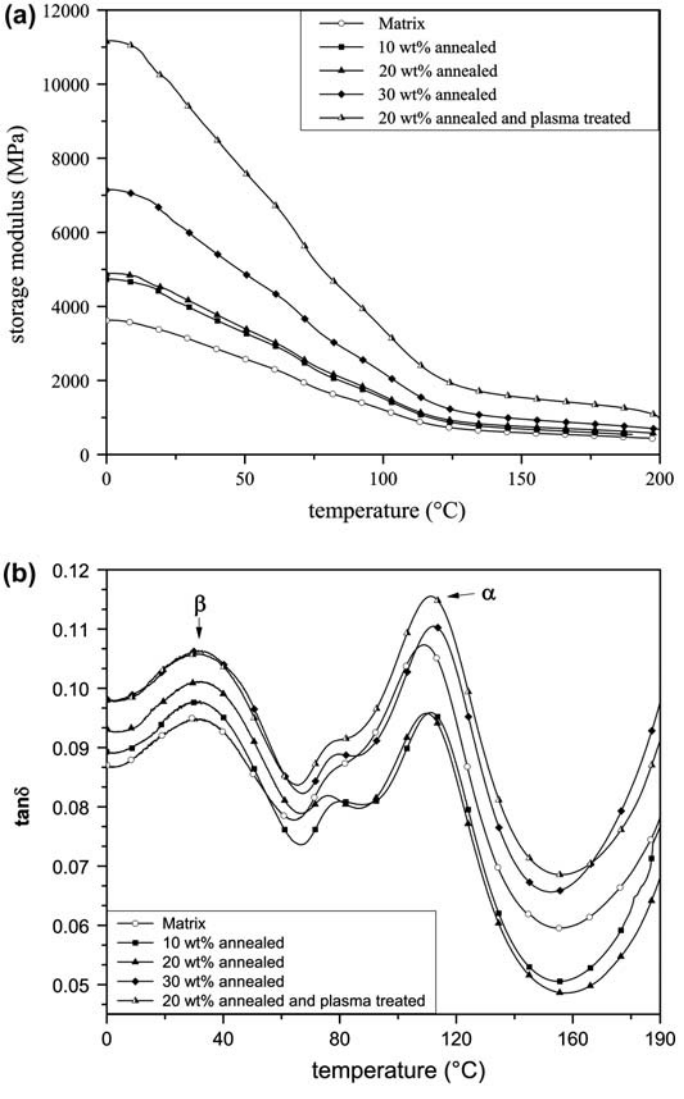

Figure 4. DMTA thermograms on SPSFCs as a function of temperature: (a) storage modulus (E') and (b) loss tangent (tan δ).

reinforcement, on the other hand, its intensity increases with the increasing fiber content. It is worthwhile to note that the α-transition slightly increases its temperature with the addition of annealed fibers.

3. Conclusions

A thermal treatment was optimized to increase the melting point and tensile properties of Vectran® NT fibers. Therefore, a processing method has been successfully developed for the production of SPSFCs. Composites containing up to 30 wt.% of thermally annealed fibers were successfully produced and a significant improvement (up to 161%) of the composite tensile modulus was observed together with a slight decrease in elongation at break was obtained. SEM observations revealed diffuse pull-out phenomena in the sample which leads us to the presence of a poor fiber–matrix interface due to the presence of sizing on the Vectran® fibers.

In order to improve the matrix–reinforcement interfacial adhesion, a surface treatment using plasma technique was performed over the heat-treated fibers. The composites using 20 wt.% of plasma-treated fibers show an increase in the elastic modulus up to 178% in comparison with the unfilled matrix. SEM observation shows fiber breakage instead of pull-out confirming the effectiveness of the plasma treatment in improving the interfacial adhesion of the composite.

References

[1] Kmetty A, Barany T, Karger-Kocsis J. Self-reinforced polymeric materials: a review. Prog. Polym. Sci. 2010;35:1288–1310.
[2] Pegoretti A. Editorial corner – a personal view. Trends in composite materials: the challenge of single-polymer composites. Express Polym. Lett. 2007;1:710.
[3] Matabola KP, De Vries AR, Moolman FS, Luyt AS. Single polymer composites: a review. J. Mater. Sci. 2009;44:6213–6222.
[4] Pegoretti A, Traina M. Liquid crystalline organic fibres and their mechanical behaviour. In: Bunsell AR, editor. Handbook of tensile properties of textile and technical fibres. Cambridge: Woodhead Publishing Ltd; 2009. 354–436.
[5] Friedel G, États mésomorphes de la matiere [Mesomorphic states of matter]. In: Proceedings of the Annales de Physique; 1922.
[6] Donald AM, Windle AH, Hanna S. Liquid crystalline polymers Cambridge University Press; 2006.
[7] Demus D, Goodby J, Gray GW, Spiess H-W, V. V. Handbook of liquid crystals: fundamentals. Weinheim: Wiley-VCH; 1998.
[8] Wang X, Zhou QF, Zhou Q. Liquid crystalline polymers World Scientific Pub. Co.; 2004.
[9] Pegoretti A, Zanolli A, Migliaresi C. Flexural and interlaminar mechanical properties of unidirectional liquid crystalline single-polymer composites. Compos. Sci. Technol. 2006;66:1953–1962.
[10] Pegoretti A, Zanolli A, Migliaresi C. Preparation and tensile mechanical properties of unidirectional liquid crystalline single-polymer composites. Compos. Sci. Technol. 2006;66:1970–1979.
[11] Isayev AI. Self-reinforced composites involving liquid-crystalline polymers – overview of development and applications. ACS Symp. Ser. 1996;632:1–20.
[12] Sarlin J, Tormala P. Isothermal heat-treatment of a thermotropic LCP fiber. J. Polym. Sci. Pol. Phys. 1991;29:395–405.
[13] Schneggenburger LA, Osenar P, Economy J. Direct evidence for sequence ordering of random semicrystalline copolyesters during high-temperature annealing. Macromolecules. 1997;30:3754–3758.

[14] Kalfon-Cohen E, Pegoretti A, Marom G. Annealing of drawn monofilaments of liquid crystalline polymer vectra/vapor grown carbon fiber nanocomposites. Polymer. 2010;51: 1033–1041.
[15] Sarlin J, Tormala P. Heat-treatment studies of a Tlcp fiber. J. Appl. Polym. Sci. 1993;50:1225–1231.
[16] Medeiros Araujo T, Sinha-Ray S, Pegoretti A, Yarin AL. Electrospinning of a blend of a liquid crystalline polymer with poly(ethylene oxide): Vectran nanofiber mats and their mechanical properties. J. Mater. Chem. C. 2013;1:351–358.
[17] Menczel JD, Collins GL, Saw SK. Thermal analysis of Vectran® fibers and films. J. Therm. Anal. 1997;49:201–208.
[18] Kalfon-Cohen E, Marom G, Wachtel E, Pegoretti A. Characterization of drawn monofilaments of liquid crystalline polymer/carbon nanoparticle composites correlated to nematic order. Polymer. 2009;50:1797–1804.
[19] Taylor JE, Romo-Uribe A, Libera MR. Molecular orientation gradients in thermotropic liquid crystalline fiber. Polym. Adv. Technol. 2003;14:595–600.
[20] Tsai SW, Pagano NJ. Composite materials workshop. Stamford, (CT): Technomic; 1968.
[21] Cox HL. The elasticity and strength of paper and other fibrous materials. Br. J. Appl. Phys. 1952;3:72–79.
[22] Loewenstein KL. Composite Materials. New York: Holliday and Elsevier; 1966.
[23] Halpin JC, Kardos JL. Halpin-Tsai equations – review. Polym. Eng. Sci. 1976;16:344–352.
[24] Pegoretti A, Ricco T. Fatigue fracture of neat and short glass fiber reinforced polypropylene: effect of frequency and material orientation. J. Compos. Mater. 2000;34:1009–1027.
[25] Blumentritt BF, Vu BT, Cooper SL. Mechanical properties of discontinuous fiber reinforced thermoplastics. II. Random-in-plane fiber orientation. Polym. Eng. Sci. 1975;15:428–436.
[26] Christensen RM, Waals FM. Effective stiffness of randomly oriented fibre composites. J. Compos. Mater. 1972;6:518–535.
[27] Kalika DS, Yoon DY. Dielectric relaxation studies of poly(4-hydroxybenzoic acid) and copolyesters based on 4-hydroxybenzoic acid and 6-hydroxy-2-naphthoic acid. Macromolecules. 1991;24:3404–3412.